Chemistry in Evaporating Ices – Unexplored Territory

Cesare Cecchi–Pestellini

INAF – Osservatorio Astronomico di Cagliari, Strada n.54, Loc. Poggio dei Pini, 09012 Capoterra (CA), Italy

ccp@ca.astro.it

Jonathan M. C. Rawlings

University College London, Department of Physics and Astronomy, Gower Street, London WC1E 6BT

jcr@star.ucl.ac.uk

Serena Viti

University College London, Department of Physics and Astronomy, Gower Street, London WC1E 6BT

sv@star.ucl.ac.uk

David A. Williams

University College London, Department of Physics and Astronomy, Gower Street, London WC1E 6BT

daw@star.ucl.ac.uk

ABSTRACT

We suggest that three–body chemistry may occur in warm high density gas evaporating in transient co–desorption events on interstellar ices. Using a highly idealised computational model we explore the chemical conversion from simple species of the ice to more complex species containing several heavy atoms, as a function of density and of adopted three–body rate coefficients. We predict that there is a wide range of densities and rate coefficients in which a significant chemical conversion may occur. We discuss the implications of this idea for the astrochemistry of hot cores.

Subject headings: astrochemistry – ISM: molecules – ISM: clouds

1. Introduction

Hot cores are well–known as sites of relatively complex chemistry in the interstellar medium (see, e.g., Snyder 2006 for a discussion of Sgr B2 N–LMH). None of these species is readily formed in conventional gas–phase chemistry under typical conditions of interstellar clouds nor of those pertaining in hot cores (number densities $n_{\rm H_2} \sim 10^7$ cm^{-3}, and temperatures $T \sim 200 - 300$ K). Attention has therefore focused on interstellar ices as a potential source of these relatively complex species. Laboratory experiments have shown that irradiation of ices of similar composition by fast particles or short wavelength electromagnetic radiation can induce greater chemical complexity to arise in the ices (e.g., Öberg et al. 2008). Concurrently, extremely detailed computational models by Herbst, Garrod, and their collaborators (e.g., Garrod, Widicus Weaver & Herbst 2008) predict that a rich and relatively complex chemistry can slowly arise in the low temperature ices. Then, when the ices are evaporated in the very dense and warm gas in the vicinity of a newly–forming star, these complex molecules are released to the gas phase and can be detected as hot core molecules.

In this work, we suggest an alternative approach that may work in parallel with these chemistries to form the large organic molecules detected in hot cores. We ask: can three–body gas–phase chemistry in high density transient events on evaporating ices create complex molecules? In the process of becoming a hot core, material warms up over a finite period of time from a low temperature (around 10 K) to about 200 K; laboratory experiments (Collings et al. 2004) show that desorption occurs in several distinct and narrow temperature bands, of which the most important for our present purposes is the so–called co–desorption band. This band is when the major component of the ice, H_2O, desorbs and carries with it all other species. This understanding of desorption has been shown to be consistent with current observations of hot cores (Viti et al. 2004).

In the picture we present here, we assume that during the warm–up of a pre–protostellar core a major part of the ices is abruptly converted during the co–desorption event from solid phase to gas phase. A truly instantaneous conversion from solid to gas would create a gas with a number density similar to that of the solid, i.e. about 10^{23} cm^{-3}. However, it is unlikely that the gas attains such high densities, but it is nevertheless possible that the density is initially at a very high level indeed, although for a very short period of time. It is our purpose here to explore whether three–body reactions in extremely dense and fairly warm gas can create molecules with complexity similar to those observed to exist in hot cores. The source species available for these chemical syntheses are assumed to be those molecules available in unprocessed interstellar ices. Can we use H_2O, CO, CH_4, etc., to create molecules of greater complexity in a highly transient and extremely dense phase?

Ideas of a similar kind were first explored by Duley (2000) who suggested that amino

acids, peptides, and a variety of organometallic compounds could be created from evaporating ices confined within cavities inside aggregate grains. Later Cecchi–Pestellini et al. (2004) computed radiation field intensities within such cavities, and suggested that prebiotic molecules might arise in the chemistry promoted in those cavities. The processes described in these papers would take place over long intervals of time during the lifetime of the core gas. In this paper, by contrast, we consider whether the conversion from chemical simplicity to chemical complexity can occur very rapidly within the transiently very high density gas arising during the evaporation of ices in the co–desorption phase. Of course, the processes discussed by Duley (2000), by Cecchi–Pestellini et al. (2004), and by Garrod, Widicus Weaver & Herbst (2008), and the ideas presented here, are not mutually exclusive.

In Section 2 we describe the physical and chemical models that we have adopted. The evaporating gas is assumed to be initially at a very high density (treated as a free parameter) and to expand either freely into a vacuum, or more slowly if there is some partial confinement of the gas by the dust grain geometry. The chemistry that we adopt is hypothetical, since there is little information available about three–body gas phase chemistry at exceptionally high number densities. Our work, therefore, is intended to be a feasibility study exploring a hitherto highly transient region of parameter space. We present in Section 3 the results of our computational modelling. Our conclusions are given in Section 4.

2. The model

2.1. The initial chemical conditions

The composition of interstellar ices, measured along different sight–lines, varies significantly (e.g., Whittet 2002; Gibb et al. 2004; Boogert et al. 2004). We adopt a composition within the observed range. The precise composition is unimportant for our present purposes, where order–of–magnitude abundances of product molecules are adequate. We assume that the instantaneously sublimated ice mantle has a typical composition as given in Table 1. For our feasibility study we currently ignore other species, whose abundances are less than 1% of the mantle composition. We also do not include CO_2, which has a typical relative abundance of 20%, on the assumption that it is tightly bound and unreactive in the assumed conditions.

2.2. The chemical network

With this limited species set, the likely reaction channels are also somewhat restricted. As the composition of the evaporating gas is dominated by H_2O and, to a lesser extent, by CO we assume that the third body in the three–body reactions is H_2O.

Three–body reactions are believed to have important roles in astronomy. They determine the chemistry in planetary atmospheres; for example, the reaction between molecules

$$CH_4 + H_2O + M \rightarrow CO + 3H_2 + M$$

(where M is a third body) may affect the deep water abundance on Jupiter (Visscher et al. 2010). The same authors also suggest that the reaction

$$H_2 + H_2CO + M \rightarrow CH_3 + OH + M$$

may open the way to radical formation (in the present work, we have excluded radical formation and reaction). Similarly, three–body reactions play a role in cool stellar atmospheres (Tsuji 1973) in the formation of simple species such as H_2, CO, CO_2, CH_4, NH_3, C_2H_2, etc. Three–body reactions also play a role in surface chemistry such as that described by Garrod, Widicus Weaver & Herbst (2008) (see also Hasegawa, Herbst & Leung 1992; Tielens & Hagen 1982; Allen & Robinson 1977). These surface chemistries invoke radical/molecule reactions in which the surface is the third body. It should be noted that all the above chemistries rely almost entirely on theoretical estimates rather than laboratory determinations.

Our proposal is that three–body reactions between molecules (rather than radical/molecule reactions) may generate a product channel of astronomical interest. Such a channel would depend on bond–breaking and atomic rearrangement, and could be driven by the high energy tail of the Boltzmann distribution in the evaporating gas. Examples of this kind of reaction that might be possible are those quoted above for Jupiter, or an alternative channel

$$CH_4 + H_2O + M \rightarrow CH_3OH + 2H + M$$

possibly followed by

$$CH_3OH + CO + M \rightarrow CH_3COOH + M$$

An interesting pair of similar reactions is quoted in the NIST database[1]

$$H_2O + CO + M \rightarrow HCOOH + M$$

[1]http://webbook.nist.gov/

followed by

$$HCOOH + H_2O + M \rightarrow HOCH_2OOH + M$$

Thus, it appears that reactions of the type we consider here are under consideration in various applications. We therefore assume that three–body reactions may occur between molecular species such as those of the initial composition.

We do not claim to know what the products of the various reactions are; we only hypothesise that non–defined complex organic molecules (which we label P_1 to P_{26}) may be formed. Obviously, this is highly simplistic and does not include the possibility of complex branching ratios, or the other (small species) products of the reactions. It therefore follows that we cannot track the abundances of the parent species with any degree of accuracy and, once the model indicates that their abundances are reduced through conversion into more complex molecules, then the model breaks down.

We have considered various types of possible three–body reactions. Normally, one thinks of the process as one that involves a chemical reaction between two species. The third body, which is chemically inert, then collisionally stabilises the excited product of this reaction. However, we can also envisage reactions in which all three species are chemically active. The reactions in this category are listed in Table 2. As stated above, we assume that H_2O is always a partner in these reactions.

The more usual formation channels would involve one of the three reactants as a chemically passive partner. Thus to obtain the products P_1 to P_{15} above would require two stages of reaction, involving intermediate species (P_{16} to P_{26}) after the first stage. These, first stage, reactions are listed in Table 3. Again, the third (now passive) partner in these reactions is taken to be H_2O.

The second stage reactions, resulting in the formation of P_1 to P_{15}, are given in Table 4. Note that we further assume that the sequence of reactions to form a product is not important; thus reaction 16 followed by reaction 27 is completely equivalent to reaction 22 followed by reaction 47.

This could be extended to include reactions between less abundant species (e.g., CH_4 and OCN^- etc.) but the products of these reactions would obviously be less abundant than the products considered here. We shall ignore these minor routes.

The rate coefficients for these various reactions are entirely hypothetical as no detailed information is available for any of the reactions in our list. We assume that the temperature dependences of the rate coefficients can be described by the usual Aarhenius formalism

$$k = k_0 \, (T/300 \text{ K})^{\alpha} \exp(-\beta/T) \qquad (1)$$

For the purposes of this exploratory calculation we assume that all reactions have the same basic rate coefficients k_0. By referring to existing databases of three–body reactions (e.g. RATE06, Woodall et al. 2007) it is evident that most of the values of k_0 for the reactions lie in the range $10^{-27} - 10^{-32}$ cm^6 s^{-1}. The values of α typically lie between 0 and -3, whilst the β values are very variable, and are quite often negative for the temperature range for which a fit is given. We consider two possible values for α: 0 and -2. So as to avoid excessive degeneracy in the parameters we set β to zero and vary k_0 to incorporate the effects of a possible barrier. Any particular value of the rate coefficient can be re–interpreted in terms of a canonical value of k_0 together with a particular value of β (see Section 4).

These are the only reactions in our chemical network; at the densities that we are considering, photoreactions and cosmic–ray ionization reactions are entirely negligible and so have been omitted.

2.3. The Physical Model

We can estimate very roughly the expected timescale for significant conversion of reactant species into complex organics on the assumptions that (*i*) there are no significant activation energy barriers to the reactions in question, and (*ii*) the reactions are generally constructive – that is to say at least one the products is more complex than the reactant species. If the density is taken to be $n \sim 10^{23}$ cm^{-3}, the rate coefficients are all 10^{-30} cm^6 s^{-1}, and the fractional abundance of the reactants (e.g., CH_4, OCN^- etc.) is of the order of 10^{-2}, then the timescale for conversion is

$$\tau \sim \frac{1}{k \times (10^{-2} n)^2} \sim 10^{-12}\,\mathrm{s}. \tag{2}$$

Therefore, the chemistry is very rapid indeed. So long as this timescale is very much less than the dynamical timescale, then the details of the expansion and cooling of the gas are of minimal relevance; essentially the chemistry takes place very shortly after the sublimation of the ice mantles when the gas density is highest; the relative abundances of the product molecules are then "frozen in" to the flow. These qualitative conclusions are confirmed by the detailed results presented in Section 3.

We consider a sphere of ice, instantaneously sublimated into the gas–phase, of initial radius r_0 and density $n_0 = 10^{23}$ molecules cm^{-3} which expands into a vacuum at some fraction, ϵ, of the sound speed v_s. The parameter ϵ allows for deviations from completely free, spherically symmetric, expansion ($\epsilon = 1$) so that a value of $\epsilon = 0$ would correspond to the situation of perfect trapping of the gas in a cavity. Thus, by mass conservation

$$n_0 r_0^3 = n r^3 = n(r_0 + \epsilon v_s t)^3 \tag{3}$$

so

$$\frac{n}{n_0} = \left(\frac{r_0}{r_0 + \epsilon v_s t}\right)^3 . \tag{4}$$

If r_0 is assumed to be comparable to the typical thickness of an ice mantle on a dust grain, then $r_0 = 10^{-5}$ cm, $v = 10^4$ cm s^{-1} and so the evolution of number density would in this case be given by

$$n/n_0 = 1/\left(1 + 10^9 \epsilon t\right)^3 \tag{5}$$

The initial temperature of the gas, T_0, is unknown as is the way that it varies with time. We are guided here by the observational results that indicate hot core temperatures of a few hundred Kelvin. The intial temperature may be higher, so we examine the temperature sensitivity up to 500 K.

For an ideal gas expanding into a vacuum (Joule expansion) the temperature would be independent of time. For adiabatic expansion, $TV^{\gamma-1}$ = constant. Thus, for spherical expansion of a gas with $\gamma = 4/3$, $T \propto r^{-1}$. In reality, the gas will cool as a result of work against intermolecular forces. In our model we consider limiting cases of

$$T = T_0 \left(\frac{r_0}{r}\right)^q \tag{6}$$

where $q = 0$ or 1. The various free parameters in our model are listed in Table 5 together with the range of values that we have investigated. For most of our model calculations we use the following values: $T_0 = 100$, $q = 0$, $\alpha = 0$, $\epsilon = 1$, with k_0 and n_0 variable. We also generally assume that the third reactant is passive (A_3 = off, see Table 5)

We calculate the time–dependences of the chemical models using a simple model, based around the GEAR integration package. Although the three–body reaction network and the extremely high densities are most unlike those applicable to models of molecular clouds, the principles are the same. As there are no variations in the chemical rate coefficients, the resultant sets of differential equations are not numerically stiff.

3. Results

The general characteristics of the results are illustrated in Tables 6 and 7 for the case of $n_0 = 10^{21}$ cm^{-3}, $T_0 = 500$ K, $k_0 = 10^{-33}$ cm^6 s^{-1}, $T \propto 1/r$ ($q = 1$), $\epsilon = 1$, $\alpha = -2$ and A_3 = off.

As can be seen from Table 6, in this model the temperature falls from its initial value to 200 K by about 10^{-9} s. The parent molecules show a slight loss in relative abundance over this period and then remain constant. Conversely, we see in Table 7 that product molecules grow

rapidly in relative abundance during a period of less than 10^{-10} s and achieve steady–state within about 10^{-9} s. The steady–state abundances depend on the two–stage chemistry and on the relative abundances of the parent species. We emphasise that it is assumed that all rate coefficients are the same and have the same temperature dependences, so there is no selectivity in the chemistry other than that introduced by the network and the initial parent abundances. In this particular example, products P_1 – P_5 attain abundances relative to H_2O of about 10^{-4}, products P_6 – P_{15} reach about 10^{-5}, while products P_{16} – P_{26} are in the range $10^{-2} - 10^{-3}$. We note at this point that an abundance of 10^{-5} relative to H_2O may correspond to a column density in a typical hot core of about 10^{15} cm^{-2}. We return to this point in Section 4.

An important feature of the model whose results are given in Tables 6 and 7 is that the chemistry is dominated by reactions occurring at the very highest densities and earliest times. Therefore, the relative chemistry arising from these reactions is essentially unchanged during the later expansion and may be said to be "frozen–in" to the expanding gas. The dominance of the early time in the chemistry (at least, for this model) also means that the dependence of the gas temperature on the expansion time (or radius) is fairly unimportant; this is also the case for the dependence of the rate coefficient on temperature. For example, for the case reported in Tables 6 and 7, if all the temperature dependences are removed then the relative abundances are not significantly changed. In what follows, we shall ignore all temperature dependences.

Clearly, the assumed initial temperature, T_0, may influence the model results. In fact, a change in T_0 from 500 K (as in Table 2) to 100 K makes only rather slight changes in the relative abundances. In the model whose results are shown in Tables 6 and 7, $k \propto T^{-2}$. The most significant of the remaining parameters are the initial density and the rate coefficients. We have therefore explored the density/rate coefficient space, over a wide range. We plot in Figure 1 a summary of these results for the case where at least some of the product molecules have relative abundances of 10^{-5} or larger. There is a wide range of (n, k) space where chemistry meets this requirement for a trapping parameter of either 0.1 and 1.0.

For the highest density case, some chemistry occurs on timescales of about 10^{-10} s even when the rate coefficient is as low as 10^{-41} cm^6 s^{-1}; we find that products P_{16} – P_{26} have relative abundances in this case of $10^{-6} - 10^{-7}$. We interpret the rate coefficient for these small values by assuming that it has a form proportional to $\exp(-\beta/T)$ (see equation 1), where β is a barrier height. Then

$$\beta = T \ln (k_0/k) \, . \tag{7}$$

If $k_0 = 10^{-31}$ cm^6 s^{-1} (a plausible value), then the barrier height for $T = 100$ K implied by a rate coefficient of 10^{-41} cm^6 s^{-1} is 2300 K, a typical barrier height for bond–breaking

of an H–X bond (see Section 4).. For the lower densities, then the value of k required to produce a significant chemistry is of course much larger. For example, at an initial density of 10^{20} cm^{-3} with zero temperature dependence, a value of $k = 10^{-31}$ cm^6 s^{-1} produces relative abundances of products P_1 – P_{15} of $10^{-5} - 10^{-6}$. A value of 10^{-31} cm^6 s^{-1} implies a barrier height of less than 500 K, which may be implausible. At an even lower initial density of 10^{17} cm^{-3}, then even the maximum plausible value of k, 10^{-29} cm^6 s^{-1}, fails to produce product molecule relative abundances larger than 10^{-6}.

The effect of changing the gas expansion parameter, ϵ, from its free expansion value of 1 to a value of 0.1 that may represent a hindered expansion from a partially enclosed cavity, may also be considered. This reduction in ϵ has the effect of maintaining the gas at the highest density for a longer time, so that the effect is allow the chemistry to proceed more quickly. For example, we compare the case of gas at a density of 10^{22} cm^{-3} where all rate coefficients are 10^{-37} cm^6 s^{-1}. For this case, the product molecules range over four orders of magnitude in relative abundances. In all cases, the relative abundance of a particular product molecule is larger by one order of magnitude when the evaporation is restricted. This behaviour is also recovered for a case with lower density, 10^{21} cm^{-3} in which some products are present with near–zero abundances.

4. Discussion and Conclusions

There are a number of general conclusions that may be drawn from this feasibility study:

1. since the density falls rapidly in the evaporating gas, the chemistry is dominated by reactions occurring at the very earliest phases, typically within about 10^{-10} s, and remains "frozen–in" at later times; if reactions work – i.e. if activation barriers can be overcome – then the chemistry will be fast and efficient;

2. as a consequence, any assumed temperature evolution in the gas is unimportant, and any assumed temperature–dependence in the adopted rate coefficients is also of little consequence;

3. therefore, the dominating parameters are the initial gas number density, n_0, and the adopted three–body rate coefficients, k;

4. the (n, k) parameter space explored includes a large region in which the complex chemistry is rich enough to be observationally significant; i.e. where complex products have an abundance relative to water of about 10^{-5}, which could be relevant for hot core

chemistry. The region of (n, k) parameter space in which this occurs is indicated schematically in Fig.1;

5. assuming that the form of the rate coefficients is

$$k = k_0 \, (T/300 \text{ K})^{\alpha} \exp{(-\beta/T)} \tag{8}$$

where β is the barrier height in Kelvins for the assumed reactions, then, if k_0 is assumed to have a canonical value of 10^{-30} cm^6 s^{-1}, the range in k of $10^{-30} - 10^{-41}$ cm^6 s^{-1} corresponds to a range in β of 0 to 2530 K if the gas temperature is about 100 K; this range in β is plausible for simple bond–breaking reactions, if the barrier height is roughly about 5% of the bond energy (Glasstone, Laidler & Eyring 1941);

6. an important conclusion is that there is a limit to chemical complexity imposed by the very short timescale available; for the range of parameters investigated here, this complexity corresponds to molecules containing about three or four heavy atoms (C, N, O); larger species are not expected from the mechanism described here;

7. if the ionization level is even slightly enhanced from zero (by some suitable process, not considered here) then the rates an conversion efficiencies may be significantly higher; similarly, if radicals were to be introduced into the expanding gas (a process not considered here), then a chemistry of the kind originally envisaged by Allen & Robinson (1977) may occur.

The overall conclusion is this: we have demonstrated a proof of concept that a rich chemistry may occur in gas evaporating from a chemically–mixed ice in the co–desorption event, assuming that the event is sufficiently narrow in temperature for very high gas densities to be achieved in the evaporate. A similar conclusion may be made for other desorption events, such as the so–called 'volcano' event, but the composition of the evaporating gas and the products would be different.

The results from this very preliminary work are of course higly tentative, but do seem to indicate, firstly, that there could be astronomical consequences from this idea, and, secondly, that further study of the idea (and of competing ideas involving three–body chemistry) probably cannot be made theoretically and would require laboratory investigation.

We may crudely regard any chemistry that generates product molecules at about 10^{-5} relative to H_2O as potentially important from the astronomical point of view. Hot cores are usually assumed to have about 1000 visual magnitudes of extinction, corresponding approximately to a column density of hydrogen of about 10^{24} cm^{-2} (e.g., Millar & Hatchell 1998). The available oxygen is mainly divided between CO (formed in the gas phase in

the early stage of the gravitational collapse of the star–forming core) and H_2O (formed by hydrogenation of O–atoms at the surface of dust and retained there as the ice mantle). The column density of each species (i.e. CO and H_2O) for hot cores in the Milky Way will be on the order of 10^{20} cm^{-2}. Therefore, molecules with an abundance relative to water of 10^{-5} may be expected to have column densities around 10^{15} cm^{-2}. The typical column density range of organic molecules in LMH is $10^{15} - 10^{16}$ cm^{-2} (Snyder 2006); for example amino acetonitrile (NH_2CH_2CN) with a column density of 2.8×10^{16} cm^{-2} (Belloche et al. 2008), and ethyl formate (C_2H_5OCHO) with a column density of 5.4×10^{16} cm^{-2} (Belloche et al. 2009). For an extended review of complex organics in interstellar clouds see Herbst & van Dishoeck (2009).

Snyder (2006) also emphasises that those molecules are hydrogen–poor. That seems likely to be the case for molecules arising in the processes considered here, as H–atoms will be ejected in the bond–breaking and bond–making processes of three–body chemistry. Indeed, the values of the rate coefficient that seem appropriate in this model do seem to imply bond–breaking of bonds of energies a few eV, i.e., corresponding to bonds involving H–atoms. We suggest that an experimental investigation be made to test the validity of the ideas expressed here.

We would like to thank the Royal Society for funding an exchange programme between UCL and Cagliari Observatory. We thank Professor S. Price and Dr W. Brown for a very helpful discussion of the ideas in this paper. We thank the referee for helpful comments that improved an earlier version of this paper.

REFERENCES

Allen M. & Robinson G.W., 1977, ApJ, 212, 396

Belloche A., Menten K.M., Comito C., Müller H.S.P., Schilke P., Ott J., Thorwirth S. & Hieret C., 2008, A&A, 482, 179

Belloche A., Garrod R.T., Müller H.S.P., Menten K.M., Comito C. & Schilke P., 2009, A&A, 499, 215

Boogert et al., 2004, ApJS, 154, 359

Cecchi–Pestellini C., Scappini F., Saija R., Iatì M.A., Giusto A., Aiello S., Borghese F. & Denti P., 2004, Int. J. Astrobiology, 3, 287

Collings M.P., Anderson M.A., Chen R., Dever J.W., Viti S., Williams D.A. & McCoustra M.R.S., 2004, MNRAS, 354, 1133

Duley W.W., 2000, MNRAS, 319, 791

Garrod R.T., Widicus Weaver S.L. & Herbst E., 2008, ApJ, 682, 283

Gibb E.L., Whittet D,C.B., Boogert A.C.A. & Tielens A.G.G.M., 2004, ApJS, 151, 35

Glasstone S, Laidler K.J. & Eyring H., 1946, Theory of Rate Processes, New York, McGraw–Hill Book Company

Hasegawa H., Herbst E. & Leung C.M., 1992, ApJS, 82, 167

Herbst E. & van Dishoeck E.F., 2009, ARA&A, 47, 427

Millar T.J. & Hatchell J., 1998, Fa. Di., 109, 15

Öberg K.I., Garrod R.T., van Dishoeck E.F. & Linnartz H, 2009, A&A, 504, 891

Snyder E., 2006, Proc. Natl Ac. Sci., 103, 12243

Tielens A.G.G.M. & Hagen W., 1982, A&A, 114, 245

Tsuji T., 1973, A&A, 23, 411

Viti S., Collings M.P., Dever J.W., McCoustra M.R.S., Williams D.A., 2004, MNRAS, 354, 1141

Whittet D.C.B., 2002, Dust in the Galactic Environment, 2nd edition, Institute of Physics Publishing, Bristol

Woodall J., Agúndez M., Markwick–Kemper A.J. & Millar T.J., 2007, A&A, 466, 1197

Visscher C., Moses J.I. & Saslow S.A., 2010, Icarus, 209, 602

Table 1: Initial gas–phase composition[(a)], relative to H_2O (100) (Whittet 2002)

Species	Abundance
H_2O	100
CO	15
CH_4	4
H_2CO	3
CH_3OH	3
NH_3	1
OCN^-	$\lesssim 1$

[(a)] We do not include CO_2 in the chemistry, as we regard that species as chemically inert in this context.

Table 2: Postulated reactions between three active partners

Number	Reaction						
1	CO	+	CH_4	+	H_2O	→	P_1
2	CO	+	OCN^-	+	H_2O	→	P_2
3	CO	+	H_2CO	+	H_2O	→	P_3
4	CO	+	CH_3OH	+	H_2O	→	P_4
5	CO	+	NH_3	+	H_2O	→	P_5
6	CH_4	+	OCN^-	+	H_2O	→	P_6
7	CH_4	+	H_2CO	+	H_2O	→	P_7
8	CH_4	+	CH_3OH	+	H_2O	→	P_8
9	CH_4	+	NH_3	+	H_2O	→	P_9
10	OCN^-	+	H_2CO	+	H_2O	→	P_{10}
11	OCN^-	+	CH_3OH	+	H_2O	→	P_{11}
12	OCN^-	+	NH_3	+	H_2O	→	P_{12}
13	H_2CO	+	CH_3OH	+	H_2O	→	P_{13}
14	H_2CO	+	NH_3	+	H_2O	→	P_{14}
15	CH_3OH	+	NH_3	+	H_2O	→	P_{15}

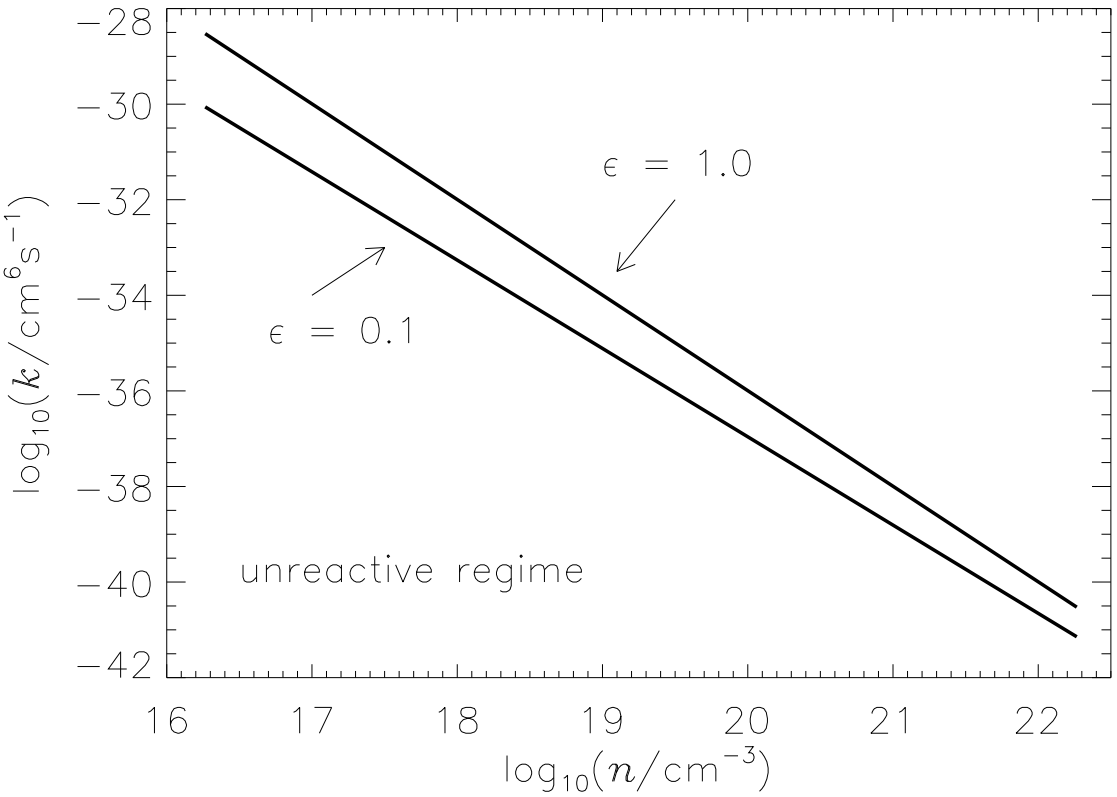

Fig. 1.— The region above the lines indicate the values of n and k for which some products have abundances larger than 10^{-5} relative to H_2O, for a model in which $T_0 = 100$ K, $q = 0$, and $\alpha = 0$. When the expansion is partially hindered, $\epsilon = 0.1$, the chemistry is faster.

Table 3: Postulated reactions between two active and one passive partner: Stage I

Number	Reaction						
16	CO	+	H_2O	+	H_2O	→	P_{16}
17	CH_4	+	H_2O	+	H_2O	→	P_{17}
18	OCN^-	+	H_2O	+	H_2O	→	P_{18}
19	H_2CO	+	H_2O	+	H_2O	→	P_{19}
20	CH_3OH	+	H_2O	+	H_2O	→	P_{20}
21	NH_3	+	H_2O	+	H_2O	→	P_{21}
22	CO	+	CH_4	+	H_2O	→	P_{22}
23	CO	+	OCN^-	+	H_2O	→	P_{23}
24	CO	+	H_2CO	+	H_2O	→	P_{24}
25	CO	+	CH_3OH	+	H_2O	→	P_{25}
26	CO	+	NH_3	+	H_2O	→	P_{26}

Table 4: Postulated reactions between two active and one passive partner: Stage II

Number	Reaction						
27	P_{16}	+	CH_4	+	H_2O	→	P_1
28	P_{16}	+	OCN^-	+	H_2O	→	P_2
29	P_{16}	+	H_2CO	+	H_2O	→	P_3
30	P_{16}	+	CH_3OH	+	H_2O	→	P_4
31	P_{16}	+	NH_3	+	H_2O	→	P_5
32	P_{17}	+	OCN^-	+	H_2O	→	P_6
33	P_{17}	+	H_2CO	+	H_2O	→	P_7
34	P_{17}	+	CH_3OH	+	H_2O	→	P_8
35	P_{17}	+	NH_3	+	H_2O	→	P_9
36	P_{18}	+	H_2CO	+	H_2O	→	P_{10}
37	P_{18}	+	CH_3OH	+	H_2O	→	P_{11}
38	P_{18}	+	NH_3	+	H_2O	→	P_{12}
39	P_{19}	+	CH_3OH	+	H_2O	→	P_{13}
40	P_{19}	+	NH_3	+	H_2O	→	P_{14}
41	P_{20}	+	NH_3	+	H_2O	→	P_{15}
42	P_{21}	+	CO	+	H_2O	→	P_5
43	P_{21}	+	CH_4	+	H_2O	→	P_9
44	P_{21}	+	OCN^-	+	H_2O	→	P_{12}
45	P_{21}	+	H_2CO	+	H_2O	→	P_{14}
46	P_{21}	+	CH_3OH	+	H_2O	→	P_{15}
47	P_{22}	+	H_2O	+	H_2O	→	P_1
48	P_{23}	+	H_2O	+	H_2O	→	P_2
49	P_{24}	+	H_2O	+	H_2O	→	P_3
50	P_{25}	+	H_2O	+	H_2O	→	P_4
51	P_{26}	+	H_2O	+	H_2O	→	P_5

Table 5: Free parameters in the model

Parameter	Description	Value
k_0	Rate coefficient	$10^{-29} - 10^{-41}$ cm^6 s^{-1}
α	Temperature dependence of rates ($k \propto T^{\alpha}$)	0 or -2
n_0	Initial number density	$10^{17} - 10^{23}$ cm^{-3}
ϵ	Trapping parameter	0.1 or 1.0
T_0	Initial temperature	$100 - 500$ K
q	Radial dependence of temperature ($T \propto r^{-q}$)	0 or 1
A_3	Flag to set reactions involving 3 active partners	on or off

Table 6: Results from the model described in the text. Results are shown for the reactant species and are given as the log of the species abundance relative to H_2O.

Time (sec)	Density (cm^{-3})	Temp (K)	CO	CH_4, HCN	H_2CO, CH_3OH	NH_3
7.98×10^{-11}	7.89×10^{20}	462.1	-0.86	-1.43	-1.55	-2.03
1.66×10^{-10}	6.26×10^{20}	427.7	-0.88	-1.45	-1.58	-2.05
2.59×10^{-10}	4.95×10^{20}	395.4	-0.89	-1.46	-1.59	-2.07
3.59×10^{-10}	3.94×10^{20}	366.6	-0.90	-1.47	-1.60	-2.08
4.68×10^{-10}	3.09×10^{20}	337.9	-0.90	-1.48	-1.60	-2.08
5.85×10^{-10}	2.51×10^{20}	315.4	-0.91	-1.48	-1.61	-2.09
7.11×10^{-10}	1.99×10^{20}	292.1	-0.91	-1.49	-1.61	-2.09
8.48×10^{-10}	1.55×10^{20}	268.7	-0.91	-1.49	-1.61	-2.09
9.95×10^{-10}	1.24×10^{20}	249.7	-0.91	-1.49	-1.61	-2.09
1.15×10^{-9}	9.40×10^{19}	227.3	-0.91	-1.49	-1.61	-2.09
1.33×10^{-9}	7.78×10^{19}	213.4	-0.91	-1.49	-1.61	-2.09
1.51×10^{-9}	6.05×10^{19}	196.3	-0.91	-1.49	-1.61	-2.09

Table 7: Results from the model described in the text. Results are shown for the product species and are given as the log of the species abundance relative to H_2O.

Time (sec)	P_1, P_2	P_3, P_4	P_5	P_6	P_7, P_8, P_{10}, P_{11}	P_9, P_{12}	P_{13}	P_{14}, P_{15}
7.98×10^{-11}	-4.66	-4.78	-5.08	-5.53	-5.66	-5.83	-5.78	-5.96
1.66×10^{-10}	-4.34	-4.36	-4.66	-5.11	-5.23	-5.41	-5.36	-5.53
2.59×10^{-10}	-4.04	-4.17	-4.47	-4.91	-5.04	-5.22	-5.16	-5.34
3.59×10^{-10}	-3.93	-4.06	-4.36	-4.81	-4.93	-5.11	-5.06	-5.23
4.68×10^{-10}	-3.87	-3.99	-4.30	-4.74	-4.87	-5.05	-4.99	-5.17
5.85×10^{-10}	-3.83	-3.95	-4.26	-4.70	-4.83	-5.01	-4.95	-5.13
7.11×10^{-10}	-3.80	-3.93	-4.23	-4.68	-4.80	-4.98	-4.92	-5.10
8.48×10^{-10}	-3.78	-3.91	-4.21	-4.66	-4.78	-4.96	-4.91	-5.09
9.95×10^{-10}	-3.77	-3.90	-4.20	-4.65	-4.77	-4.95	-4.90	-5.07
1.15×10^{-9}	-3.76	-3.89	-4.19	-4.64	-4.76	-4.94	-4.89	-5.07

Time (sec)	P_{16}	P_{17}, P_{18}	P_{19}, P_{20}	P_{21}	P_{22}, P_{23}	P_{24}, P_{25}	P_{26}
7.98×10^{-11}	-2.05	-2.62	-2.74	-3.22	-3.47	-3.59	-4.07
1.66×10^{-10}	-1.84	-2.41	-2.53	-3.02	-3.27	-3.40	-3.87
2.59×10^{-10}	-1.74	-2.31	-2.44	-2.92	-3.19	-3.31	-3.79
3.59×10^{-10}	-1.69	-2.26	-2.38	-2.87	-3.14	-3.27	-3.75
4.68×10^{-10}	-1.66	-2.23	-2.35	-2.84	-3.12	-3.24	-3.72
5.85×10^{-10}	-1.64	-2.21	-2.33	-2.82	-3.10	-3.22	-3.70
7.11×10^{-10}	-1.62	-2.20	-2.32	-2.81	-3.09	-3.21	-3.69
8.48×10^{-10}	-1.62	-2.19	-2.31	-2.80	-3.08	-3.21	-3.68
9.95×10^{-10}	-1.61	-2.18	-2.31	-2.79	-3.08	-3.20	-3.68
1.15×10^{-9}	-1.61	-2.18	-2.30	-2.79	-3.07	-3.20	-3.68